Proceedings of the 1999 IEEE/RSJ
International Conference on
Intelligent Robots and Systems

Time-Varying Input Shaping Technique Applied to Vibration Reduction of An Industrial Robot

Hyung-Soon Park* Pyung H. Chang* Jong-Sung Hur**

* Department of Mechanical Engineering, KAIST
373-1 Kusung-dong, Yusung-gu, Taejon, Korea
** Robotics Research Department, Hyundai Heavy Industries Co., Ltd.,
1-8, Mabook-Ri, Kuseong-Myun, Yongin-Shi, Kyunggi-Do, Korea

Abstract

It is widely and frequently observed that industrial robots conducting fast motion involve serious residual vibration, the period of which varies with time. To this problem, this paper presents a practical solution by providing a practical design and application of time-varying input shaping technique (TVIST) for an industrial robot. To suppress the time-varying vibration, at first, a guideline for designing practical TVIST is presented. Following the guideline, then, we design TVIST for a large size 6 degrees of freedom industrial robot. In doing so, a simple yet effective equation is derived from robot dynamic equations to estimate the time-varying period. Furthermore, a simple payload-adaptation scheme is also included. The TVIST thus designed is experimented on the industrial robot under spatial motion and payload variation conditions. The experimental results show that the residual vibration is reduced to less than 10% of original one in magnitude, demonstrating that the efficiency of the TVIST does not compromise its effectiveness.

Keywords : residual vibration; vibration control; industrial robot; time-varying vibration

1 Introduction

This paper presents a *practical solution* to the residual vibration problem frequently and widely found in industrial robots. Provided below are the backgound and context associated with the problem and our solution approach.

It is well known that industrial robots need to achieve higher speed and precision for better productivity. To this end, one of major obstacles to overcome is the residual vibration of the end-effector coming from joint flexibility primarily due to the transmissions on the motor axes. The residual vibrations they exhibit tend to be nonlinear and time-varying, owing to the configuration[1]-dependent inertia-variation and the nonlinear stiffness of the gears. Moreover, the vibration becomes further complicated by different payloads an industrial robot handles.

[1]By configuration we mean the robot posture determined by joint variables.

As an effective method to resolve this problem, we have considered the input shaping technique (IST). Since it was first proposed[1], the IST has attracted attentions owing to its effectiveness and simplicity. Its effectiveness has been confirmed by the application results from practical systems such as a surface mounting machine[3], a single link flexible spacecraft[4], and an open container of liquid[5]. Nevertheless, since the IST was proposed originally for linear time-invariant systems[1, 2], it is not so effective for systems with nonlinearity and time-varying characteristics. Even robust IST[1, 2], which handles inaccuracy of period estimation, is not of much help for these systems.

In response, many researchers have extended IST to nonlinear time-variant systems. Rappole[6] applied time-varying input shaping technique (TVIST) to a two-link flexible manipulator using look-up table that contains the information of configuration-dependent frequency. Magee and Book[7] modified the IST to eliminate the first two modes of vibration in a large and flexible manipulator having configuration-dependent inertia. Cho and Park[8] proposed a method for determining the exact time-varying impulse sequence for linear time-variant systems, and applied it to a two-link flexible robot. An adaptive IST was proposed for time-variant systems that uses a real-time identification scheme[9].

The aforementioned TVIST's, however, appear to be more or less theoretical in the sense that (1) they tend to be limited to highly flexible robots, rarely found in practice except for some special-purpose robots; and (2) the practical issues associated with implementation do not seem to be their immediate concerns. For instance, the look-up table scheme[6] needs to consider the size requirement and availability of memory, whereas the TVIST's[8, 9], having complicated structures, the CPU power. To our knowledge, there have been few research works that address these issues and apply TVIST to practical systems such as industrial robots.

In this paper, we present a practical design guideline for TVIST relevant to most industrial robots (in Section 2). Along the guideline, we design a TVIST for a specific robot, a large size industrial robot (in Section 3). Finally we apply the TVIST to confirm its performance through experiment (in Section 4), thereby demonstrating that we

0-7803-5184-3/99/$10.00

have provided a *practical solution* to the residual vibration problem in industrial robots.

2 Design Guideline for TVIST

The essential difference of TVIST from the IST lies in that TVIST requires real-time update of time-varying parameters: the period and damping ratio of the system. Hence, a *practical* TVIST should be able to determine *which* of the two parameters to update and *how* to do so. Accordingly, our design procedure begins with these two decision makings, as illustrated in the flowchart in Figure 1.

More specifically, we need to discern in the first place which parameter should be treated as time-varying and which parameter constant. For instance, damping ratio for most mechanical systems is closely related to the viscosity, which does not change rapidly. Consequently, the damping ratio can be assumed as a constant with respect to time, whereas the period of vibration is treated as time-varying. However, if the variation of damping ratio is not negligible, it should also be treated as a time-varying parameter, and the updating rule should be designed accordingly.

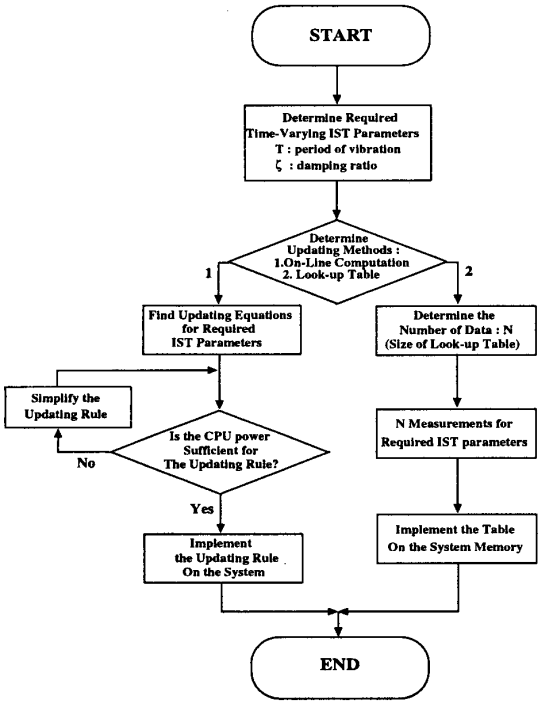

Figure 1: Flowchart for the design procedure

In the design of a practical TVIST, it is crucial to have a *reliable method* to update in real-time the time-varying parameters. The updating methods may be classified into two groups:

- A look-up table is used to provide the values of the time-varying parameters for each joint configuration[6].
- Robot dynamics model is computed on-line to obtain the values of the time-varying parameters[7, 8, 9].

Obviously, the former is appropriate for systems with sufficient memory size; the latter for systems with sufficient computational power.

In the former method, the memory size determines the number of data in the look-up table. Once the number of data is determined, the selected time-varying parameters are measured through experiments at different configurations. Finally, the data are memorized in the look-up table.

In the latter method, an analytic equation is constructed through the model of the considered plant. Then the amount required to compute the equation must be compared to the computational power of the CPU. If the CPU power is not enough to perform the real-time computation, the updating rule should be simplified to reduce the amount of computation, either by decreasing the updating rate or by simplifying the updating equation.

Table 1: Descriptions and numerical values for parameters

parameter	description	value
l_a, l_c	length of link a, link c	1.25 $[m]$
l_b	length of link b	0.5 $[m]$
l_d	length of link d	1.8 $[m]$
m_a	mass of link a	160.0 $[kg]$
m_b	mass of link b	260.0 $[kg]$
m_c	mass of link c	30.0 $[kg]$
m_d	mass of link d	260.0 $[kg]$

3 Practical Design of TVIST for the Industrial Robot

The industrial robot of our concern has a parallelogram-linkage structure with 6 degrees of freedom, the schematic diagram of which is shown in Figure 2. The descriptions and the approximated values for the parameters in Figure 2 are listed in Table 1. As the size of the robot implies, it is intended for a heavy-duty material handling or spot welding, the maximum payload of which is 120 kg. Since all the joints are of revolute type, the period of vibration varies with the configurations of the robot. From experimental observation, the period of the residual vibration varies from 125 $msec$ to 300 $msec$ within the operational range of the robot, whereas the damping ratio does not vary significantly. Hence, the period is treated as a time-varying parameter and the damping ratio is set to be constant. For the next step, an updating equation is designed for the real-time information of the period of the vibration.

As for the joint controller of the robot, it has a CPU of TMS320C25 and memory of 192 kbyte. This controller, were it used for TVIST only, would be suitable for both the look-up table and on-line computation. Yet, it turns out that most of the computation resource is used for other purposes such as safety functions, several interfaces of the robot, and so on. Since the left-over memory is not sufficient for any type of look-up table, the only option left is to

adopt the on-line computation of an updating equation in a substantially simplified form. In order to construct such an updating equation, we first derive the dynamic equation of the robot, then analyze its dynamic behavior, and finally determine a simple yet physically meaningful equation to update the period.

3.1 Dynamic Equation of the Industrial Robot

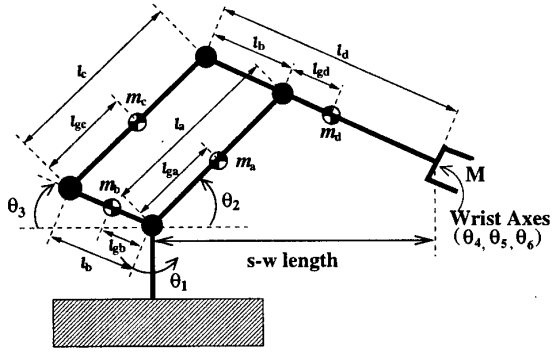

Figure 2: Schematic diagram of the industrial robot

As shown in Figure 2, the first axis, specified as the joint axis for θ_1, is the swing-axis, which rotates the overall linkage. The vertical axes, the axes for θ_2 and θ_3, determine the configuration of the parallelogram-linkage. The last three axes, the respective rotation about which are θ_4, θ_5, and θ_6, determine the orientation of the end-effector. Note that they have little effect on the inertia-variation and thus on the period-variation; therefore, the dynamic equation is derived only for the first three joints.

Since joint flexibility is considered as the primary source of robot vibration, it is included in the model. The flexibility of the i-th joint is modeled as a torsional spring with stiffness, K_{Ti}, and gear reduction, r_i[10]. Consequently, each axis includes two joint variables representing motor angle (θ_{mi}) and link angle (θ_i), as shown in Figure 3.

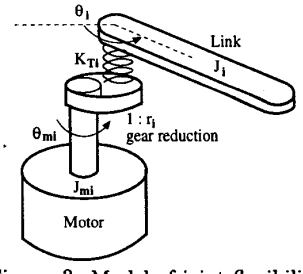

Figure 3: Model of joint flexibility

The dynamic equation of the robot is derived by using Lagrange's method and expressed as follows:

$$M_{11}\ddot{\theta}_{m1}+c_{m1}\dot{\theta}_{m1}+\frac{c_{k1}}{r_1}\left(\frac{\dot{\theta}_{m1}}{r_1}-\dot{\theta}_1\right)+\frac{K_{T1}}{r_1}\left(\frac{\theta_{m1}}{r_1}-\theta_1\right)=\tau_1 \quad (1)$$

$$M_{22}\ddot{\theta}_1+c_1\dot{\theta}_1-c_{k1}\left(\frac{\dot{\theta}_{m1}}{r_1}-\dot{\theta}_1\right)-K_{T1}\left(\frac{\theta_{m1}}{r_1}-\theta_1\right)+N_1(\boldsymbol{\theta},\dot{\boldsymbol{\theta}})=0 \quad (2)$$

$$M_{33}\ddot{\theta}_{m2}+c_{m2}\dot{\theta}_{m2}+\frac{c_{k2}}{r_2}\left(\frac{\dot{\theta}_{m2}}{r_2}-\dot{\theta}_2\right)+\frac{K_{T2}}{r_2}\left(\frac{\theta_{m2}}{r_2}-\theta_2\right)=\tau_2 \quad (3)$$

$$M_{44}\ddot{\theta}_2+M_{46}\ddot{\theta}_3+c_2\dot{\theta}_2-c_{k2}\left(\frac{\dot{\theta}_{m2}}{r_2}-\dot{\theta}_2\right)-K_{T2}\left(\frac{\theta_{m2}}{r_2}-\theta_2\right)+N_2(\boldsymbol{\theta},\dot{\boldsymbol{\theta}})+G_2(\boldsymbol{\theta})=0 \quad (4)$$

$$M_{55}\ddot{\theta}_{m3}+c_{m3}\dot{\theta}_{m3}+\frac{c_{k3}}{r_3}\left(\frac{\dot{\theta}_{m3}}{r_3}-\dot{\theta}_3\right)+\frac{K_{T3}}{r_3}\left(\frac{\theta_{m3}}{r_3}-\theta_3\right)=\tau_3 \quad (5)$$

$$M_{64}\ddot{\theta}_2+M_{66}\ddot{\theta}_3+c_3\dot{\theta}_3-c_{k3}\left(\frac{\dot{\theta}_{m3}}{r_3}-\dot{\theta}_3\right)-K_{T3}\left(\frac{\theta_{m3}}{r_3}-\theta_3\right)+N_3(\boldsymbol{\theta},\dot{\boldsymbol{\theta}})+G_3(\boldsymbol{\theta})=0, \quad (6)$$

where $\boldsymbol{\theta}=[\theta_1 \quad \theta_2 \quad \theta_3]^T$, $\dot{\boldsymbol{\theta}}=[\dot{\theta}_1 \quad \dot{\theta}_2 \quad \dot{\theta}_3]^T$; and $N_i(\boldsymbol{\theta},\dot{\boldsymbol{\theta}})$ denotes the Coriolis and centrifugal torque and $G_i(\boldsymbol{\theta})$ the gravity torque, at the i-th joint. In the equations above, it is assumed that viscous damping with a coefficient of c_{mi} is present at each motor, c_i at each joint, and c_{ki} at each torsional spring.

3.2 Estimation of Time-Varying Period

Because the inertia term, $M_{ij}(\boldsymbol{\theta})$, in the dynamic equation above directly influences the period of vibration, it should be examined carefully. Assuming uniform and symmetric cross-section of the links, the elements of $M_{ij}(\boldsymbol{\theta})$'s are expressed as the following.

$$M_{11}=J_{m1} \quad (7)$$

$$M_{22}=(m_a l_{ga}{}^2+J_a+J_c)c_2{}^2+(m_b l_{gb}{}^2+J_b+J_d)c_3{}^2+m_c(l_b c_3-l_{gc}c_2)^2+m_d(l_c c_2+l_{gd}c_3)^2+M(l_c c_2+(l_d-l_b)c_3)^2 \quad (8)$$

$$M_{33}=J_{m2} \quad (9)$$

$$M_{44}=m_a l_{ga}{}^2+J_a+m_c l_{gc}{}^2+J_c+m_d l_a{}^2+M l_a{}^2 \quad (10)$$

$$M_{46}=M_{64}=m_d l_a l_{gd}\cos(\theta_2-\theta_3)-m_c l_b l_{gc}\cos(\theta_2-\theta_3)+M l_a(l_d-l_b)\cos(\theta_2-\theta_3) \quad (11)$$

$$M_{55}=J_{m3} \quad (12)$$

$$M_{66}=m_b l_{gb}{}^2+J_b+m_c l_b{}^2+m_d l_{gd}{}^2+J_d+M(l_d-l_b)^2, \quad (13)$$

where l_k and l_{gk} $(k=a,b,c,d)$ denote the length of the corresponding link and the length to the center of gravity, respectively, as shown in Figure 2. In the same manner, m_k and J_k represent the mass of the link and the moment of inertia, respectively. In addition, M denotes the payload, which is attached at the end-effector; and c_2 and c_3 symbolize $\cos\theta_2$ and $\cos\theta_3$, respectively.

3.2.1 Derivation of Time-Varying Period

Since the residual vibration of each and every joint contributes to determine that of the end effector, it is necessary to estimate the period of each joint. The essence of residual vibration at each joint can be represented with a model consisting of a mass and a spring, as shown in Figure 3. The period of vibration for the i-th joint, then, can be expressed as follows:

$$T_i=2\pi\sqrt{\frac{M_{(2i)(2i)}(\boldsymbol{\theta})}{K_{Ti}}} \quad (i=1,2,3). \quad (14)$$

Note in (8) that the inertia about the swing-axis, M_{22}, varies with θ_2 and θ_3, whereas M_{44} and M_{66} have constant values. Furthermore, M_{44} and M_{66} take smaller value compared to the swing-axis and so does the magnitude of vibration. This observation implies that the *time-varying* residual vibration of the end effector is predominantly determined by that of the swing-axis. This finding is practically very important because it enables us to concentrate on the swing-axis only, designing a TVIST for it. For the rest of other axes, we can design other prefilters for time-invariant systems such as the conventional IST.

Consequently, (8) and (14) serve as *the central relationship* for the estimation of the time-varying period. In (8), in order to estimate $M_{22}(t)$, we should measure $\theta_2(t)$ and $\theta_3(t)$ in real-time. Although K_{T1} generally has nonlinear time-varying characteristics, it is assumed to be a constant based on the observation that the stiffness-variation is not substantial compared to the inertia-variation.

3.2.2 A Simplified Period Estimation

Many industrial controllers — like ours — could require more simplified equation than (8) and (14), because (8) contains sinusoidal functions, which demand more computation than a simple addition or multiplication. For the simplification, we select a simple yet effective index: *s-w length*. As shown in Figure 2, the s-w length, $x(t)$, is defined as a length from the swing-axis to the wrist-axis along horizontal line.

Considering that the inertia (M_{22}) can be approximated by an equivalent mass (M_{eq}) located at x from the swing-axis, one can expect that the period is approximately proportional to x, as follows:

$$T = 2\pi\sqrt{\frac{M_{22}}{K_{Ti}}} \approx 2\pi\sqrt{\frac{M_{eq}x^2 + C}{K_{T1}}} \propto x\,, \qquad (15)$$

where C denotes an appropriate constant for the approximation.

Although the s-w length is still the trigonometric function of the vertical angles, no additional calculation is required, because $x(t)$ usually has been already computed for other purposes such as the identification of end effector location for user-interface. As a result, (8) and (14) are simplified into (15), a linear function of $x(t)$, and the computational burden is greatly reduced.

Figure 4 shows the experimental results of our robot that the period of vibration is approximately proportional to the s-w length except for the low s-w lengths.

For the lower s-w lengths, there are more than a set of θ_2 and θ_3 due to multiple inverse kinematic solutions, resulting in different inertias, which implies that the linearity may not work at low s-w lengths. Fortunately, however, the magnitude of the vibration is sufficiently small at low s-w lengths owing to the low inertia about the swing-axis. For this reason, the approximation error is not problematic at low s-w lengths; and hence the period can safely be approximated with a linear function over the whole s-w lengths.

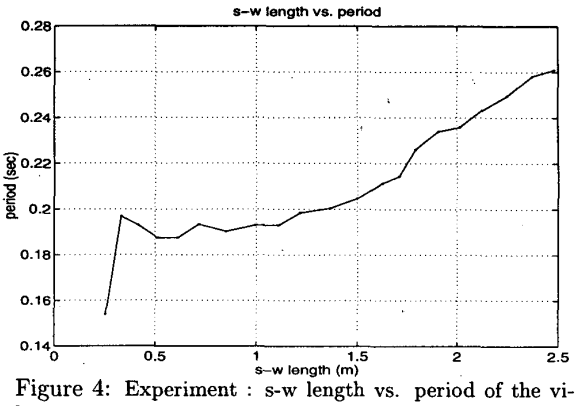

Figure 4: Experiment : s-w length vs. period of the vibration

Accordingly, given s-w length, $x(t)$, the half period is estimated as the following equation:

$$T_{half}(t) = ax(t) + b \;\; [sec]\,, \qquad (16)$$

where the coefficients are determined for our robot as $a = 0.095\ [sec/m]$ and $b = 0.0475\ [sec]$.

3.2.3 Load Variation

Normally, a robot is meant to perform various tasks demanding different payloads, M. (8) and (14) clearly show that the variation in M immediately causes to change the period. In the period estimation, thus, it is important to take this variation into account, so that the controller may be able to adjust T_{half} for a different value of M supplied by user.

The period of vibration, as (8) and (14) imply, is proportional to the square root of M; however, it is observed from experiments that the period tends to be approximately proportional to M in the operational range ($M = 20kg \sim 120kg$), as shown in Figure 5. And this tendency holds for different s-w lengths due to various configurations.

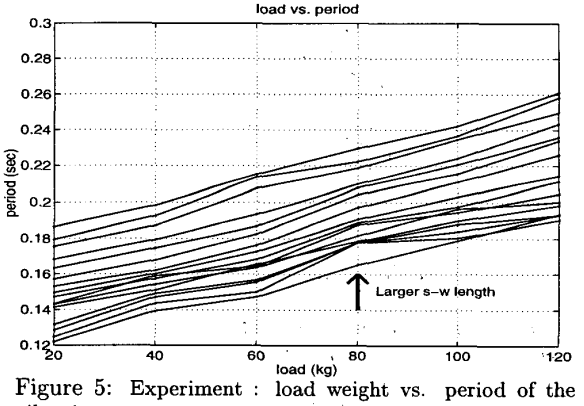

Figure 5: Experiment : load weight vs. period of the vibration

From the experimental results, (16) is modified to adapt to the payload, M, as follows:

$$T_{half}(M,t) = ax(t) + b - c(120 - M) \quad [sec]) \,, \qquad (17)$$

where $c = 0.76$ $[sec/kg]$.

(17) is our final updating equation to estimate the period of the residual vibration. Once an user inputs the payload, M, depending on a given task, (17) determines the period of time-varying residual vibration. Recollecting the derivation procedure thus far, one can find that (17) covers a broad range of industrial robots.

3.3 Final Design of TVIST

As for the implementation of TVIST, the time interval of the impulse sequence is determined from (17), and the time-varying impulse sequence is convoluted with the desired trajectory. If three impulses are implemented for the robustness[1], the TVIST is implemented for a given desired trajectory, $\theta_{1d}(t)$, as follows:

$$\begin{aligned}\theta_{1d}{}^{*}(t) = {} & A_1\theta_{1d}(t) + A_2\theta_{1d}(t - T_{half})u(t - T_{half}) \\ & + A_3\theta_{1d}(t - 2T_{half})u(t - 2T_{half}) \,, \qquad (18)\end{aligned}$$

where A_1, A_2 and A_3 are the magnitudes of each impulse and $u(t - T_{half})$ is a unit step function defined as follows:

$$u(t - T_2) = \begin{pmatrix} 0 & \text{for } t < T_{half} \\ 1 & \text{for } t \geq T_{half} \end{pmatrix} . \qquad (19)$$

As shown in [1], A_1, A_2, and A_3 are calculated from the damping ratio, which is set to constant.

4 Experimental Result

The proposed TVIST using (17) is embedded in the controller of the robot so that any additional user's interactions may not be necessary to perform various tasks. In the experiments, the vibration is measured by an accelerometer.

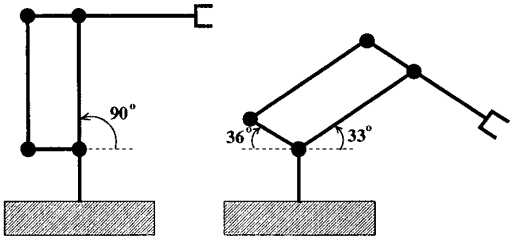

Figure 6: Two configurations of the robot

In the first experiment, we attempt to verify that the proposed TVIST works at different configurations, by testing its performances at two different configurations of vertical axes with 120 kg load attached. At each fixed configuration of θ_2 and θ_3, the swing-axis is controlled to track a given trajectory of 10° rotation.

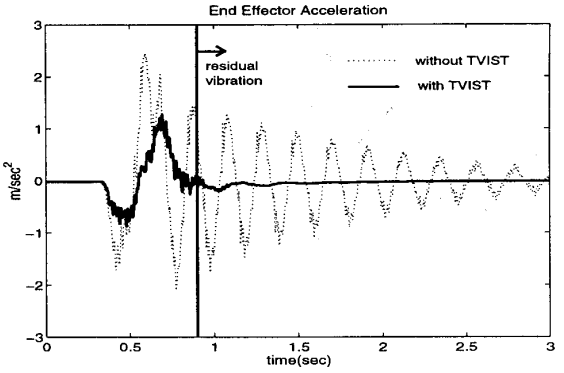

Figure 7: Experimental result at Configuration 1

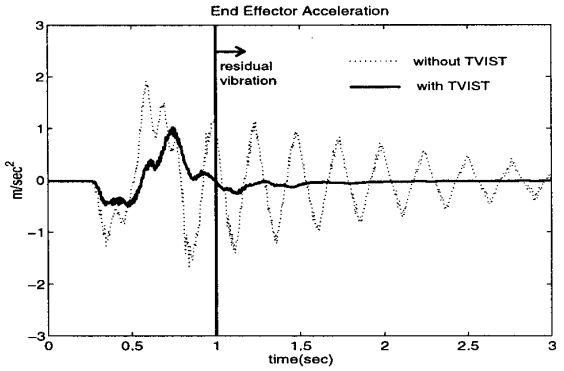

Figure 8: Experimental result at Configuration 2

When it is controlled by a feedback controller only, which is equivalent to the PID controller, the residual vibration is problematic as both Figure 7 and Figure 8 show. In Figure 7, with $\theta_2 = 90°$ and $\theta_3 = 0°$ (corresponding to Configuration 1 in Figure 6), the frequency of vibration is 5 Hz, and the frequency reduces to 3.5 Hz in Figure 8, with $\theta_2 = 33°$ and $\theta_3 = 36°$ (corresponding to Configuration 2 in Figure 7). In Figure 7 and Figure 8, the residual vibration corresponds to the right side of the bold vertical line and should not be confused with the transient response on the left side. The results show that the vibrations are reduced to 10% of their original magnitude by using the proposed TVIST. It should be noted that the proposed TVIST does not require additional tuning because it automatically estimates the period of vibration.

In the second experiment, it is tested for a motion that brings time-varying vibration. The vertical axes moves from Configuration 1 to Configuration 2 while the swing-axis rotates 50° simultaneously. The inertia about the swing-axis varies during the motion and so does the period of vibration. The result in Figure 9 shows that the proposed TVIST suppresses the residual vibration, whereas the conventional IST with the fixed parameter does not.

In the final experiment, the load-adaptability is tested. The same operation is repeated as the first experiment at Configuration 2; but, this time, with each payload of 40

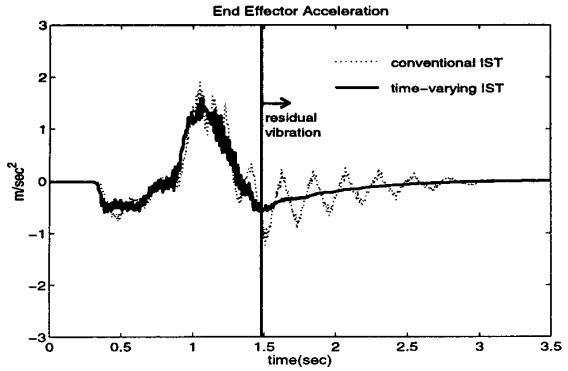

Figure 9: Experimental result at time-varying configuration (Configuration 1 to Configuration 2)

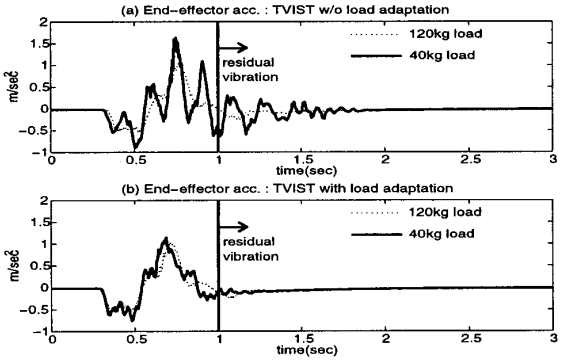

Figure 10: Experimental results with various loads

kg and 120 kg. Figure 10 shows the comparison between two TVIST's: (a) the one without load-adaptation scheme, and (b) the other with it. The latter(b) clearly suppresses vibrations with both 120 kg and 40 kg, effectively adapting to the load variation, whereas the former with a design fixed to 120 kg load does not suppress very effectively the vibration with 40 kg load.

5 Conclusion

For suppression of time-varying residual vibration in the industrial robot, a practical design procedure of TVIST is presented and the procedure is applied to an industrial robot. The updating rule of TVIST is practically designed to be computationally efficient so that it can be implemented in real-time.

In designing the TVIST, the period of vibration needs to be estimated in real-time. By using s-w length as a time-varying variable, the period of vibration at each configuration can be estimated efficiently. In addition, the TVIST is modified to adapt to the various payload. As a result, the residual vibration is reduced to less than 10 % of the original one.

Through this research, it is shown that the TVIST can be designed for practical systems without sacrificing its computational efficiency. As an example, it is shown that the TVIST works well on such a realistic system as the industrial robot even though it is simplified for computational efficiency. Recollecting that the derivation of the updating rule is readily applicable to a wide range of industrial robots, we consider that this work provides a promising example of the application of TVIST to various industrial robots.

Acknowledgments

This work is supported by Hyundai Heavy Industries Co., Ltd.

References

[1] N. C. Singer, "Residual Vibration Reduction in Computer Controlled Machines," *PhD thesis, Department of Mechanical Engineering, MIT*, Fall, 1988.

[2] N. C. Singer and W. P. Seering, "Preshaping Command Inputs to Reduce System Vibration," *ASME Journal of Dynamic Systems, Measurement and Control*, Vol. 112, pp. 76-82, 1990.

[3] P. H. Chang and J. Park, "Use of Input Shaping Technique with a Robust Feedback Control and Its Application to The Position Control of Surface Mount Machine," *Proceedings of the IEEE International Conference on Control Applications*, pp. 397-402, 1996.

[4] Q. Liu and B. Wie, "Robust Time-Optimal Control of Uncertain Flexible Spacecraft," *Journal of Guidance and Control*, Vol. 15, pp. 597-604, 1992.

[5] J. Feddema, C. Dohrmann, et al., "A Comparison of Maneuver Optimization and Input Shaping Filters for Robotically Controlled Slosh-Free Motion of an Open Container of Liquid," *CDROM of the 1997 American Control Conference*, TA01_05.pdf, 1997.

[6] B. W. Rappole, "Minimizing Residual Vibrations in Flexible Systems," *Master thesis, Department of Mechanical Engineering, MIT*, 1992.

[7] D. P. Magee and W. J. Book, "Implementing Modified Command Filtering to Eliminate Multiple Modes of Vibration," *Proceedings of the 1993 American Control Conference*, pp. 2700-2704, June 1993.

[8] J. K. Cho and Y. Park, "Vibration reduction in flexible systems using a time-varying impulse sequence," *Robotica*, Vol. 13, pp. 305-313, 1995.

[9] A. Tzes and S. Yurkovich, "An Adaptive Input Shaping Control Scheme for Vibration Suppression in Slewing Flexible Structures," *IEEE Transactions on Control Systems Technology*, Vol. 1, pp. 114-121, 1993.

[10] R. Kinceler and P. H. Meckl, "Corrective Input Shaping for a Flexible-Joint Manipulator Performing Point-to-Point Motion," *Proceedings of the IEEE International Conference on Control Applications*, pp. 391-396, 1996.